

STUDY OF SOME NUMERICAL ARTIFACTS INTERVENING IN THE FINITE DIFFERENCES SIMULATIONS OF KdV SOLITONS PROPAGATION

Ion APOSTOL¹, Dan Alexandru IORDACHE², Pier Paolo DELSANTO³,
Viorica IORDACHE⁴

Abstract. *As it is well known, the complex simulations are frequently affected by numerical artifacts, which reduce drastically their accuracy. Taking into account that the numerical artifacts due to the non-linearity of the considered physical problem are less studied than those due to the symmetry breaking or to the high logical depth of the used schemes, the finite differences (FD) simulations of some (Korteweg-de Vries) solitonic pulses were studied. In this aim, both the possible FD discretizations and the artifacts corresponding to different values of the simulation uniqueness parameters were studied. The possibilities to explain quantitatively the observed numerical artifacts, transforming them in numerical phenomena, were also studied.*

Keywords: Complex numerical simulations, numerical artifacts, Korteweg-de Vries solitary waves, FD discretizations, numerical phenomena

1. Introduction

As it is well-known, we live in a computerized world, our civilization being a “civilization of computers”. Since all complex installations and devices are now controlled by computers, their corresponding complex simulations can lead to some numerical artifacts and – if they are used to control such systems – to major failures. Particularly, the Patriot missile failure to stop a Scud missile during the Gulf War in 1991 (with disastrous results) [1] and the self-destruction of the European Space Agency’s Ariane 5 rocket, at 37 seconds after its launch [2], were both assigned to some computer errors [3] and their associated numerical artifacts. If the mechanisms of the computer artifacts installation can be quantitatively described, these artifacts are called « numerical phenomena » [4].

A typical source of numerical artifacts corresponds to the Finite Difference (FD) simulations of the solitary waves propagation, due to the nonlinear character of their equations. Taking into account the major applications of the more than 100 types of different solitary waves [5] in all Physics fields: Cosmology and Astrophysics, Mechanics and Fluid Mechanics, Molecular chains, Condensed

¹PhD student, Physics Department II, University “Politehnica” of Bucharest, Romania.

²Professor, Physics Department II, University “Politehnica” of Bucharest, Romania.

³Professor, Physics Department, Politecnico di Torino, Italy.

⁴MEng, Physics Department II, University “Politehnica” of Bucharest, Romania.

matter Physics (involving the applications for the information transmission through optical fibers [6], the Josephson (superconductive) devices, etc.), Plasma Physics, Nuclear Physics, applications in Medicine [7] etc.

A detailed analysis of numerical artifacts intervening in the FD simulations of pulses propagation [4], [8], pointed out that – for the complex simulations due to: a) the symmetry breaking and to: b) the high logical depth of the involved computer programs - their basic types are those of: (i) instability, (ii) divergence or pseudo-convergence (even more dangerous, because it produces some misleading results), (iii) distortions, etc.

The main goal of this work is to point out the specific numerical artifacts corresponding to the FD simulations associated to pulses propagation described by nonlinear equations.

2. Studied FD discretizations of the KdV equation

Starting from the one-dimensional (1D) propagation equation [9] of the Korteweg-de Vries (KdV) solitons, in terms of their non-linearity n and dispersion d coefficients, respectively, and of the unperturbed speed (in absence of the nonlinearity and dispersion properties of the propagation medium) V_{oo} :

$$\dot{y} = -V_{oo} \cdot y' - n \cdot y \cdot y' - d \cdot y''' \quad (1)$$

the studied discretization schemes are built by means of some specific FD approximations of the space derivatives y' and y''' [10]. Denoting the pulse magnitudes (in the space site i) in the past, present and future time step by means of symbols $p(i)$, $pr(i)$ and $f(i)$, there are obtained the basic KdV equation discretizations for the main studied y' and y''' FD approximations (see below).

2.1. The Landau-Pàez discretization [11]

Starting from the simplified (assuming $V_{oo} = 0$) expression of the KdV equation:

$$\dot{y} + n \cdot y \cdot y' + d \cdot y''' = 0, \quad (2)$$

the symmetric discretization:

$$f(i) = p(i) - \frac{n \cdot \tau}{3\chi} [pr(i+1) + pr(i) + pr(i-1)] \cdot [pr(i+1) - pr(i-1)] - \frac{d \cdot \tau}{\chi^3} [pr(i+2) + 2pr(i-1) - 2pr(i+1) - pr(i-2)], \quad (3)$$

(where τ and χ are the FD time and space steps, respectively) is used.

2.2. The permanent 2 steps symmetric discretization [12] (pp. 271-275)

The study of different FD discretizations pointed out that the asymmetric schemes lead quickly to the instability appearance.

For this reason and simplicity, we studied previously [11] the permanent 2 steps symmetric FD discretization:

$$f(i) = p(i) - \gamma [pr(i+1) - pr(i)] + a \cdot pr(i) \cdot [pr(i-1) - pr(i+1)] + b \cdot [pr(i-2) - pr(i+2)], \quad (4)$$

with:
$$a = \frac{n \cdot \tau}{\chi}, \quad b = \frac{d \cdot \tau}{\chi^3}, \quad \gamma = \frac{\tau}{\chi} \left(V_{00} - \frac{2n}{\chi^2} \right), \quad (5)$$

where τ and χ have the same meaning (FD time and space steps, respectively).

Given being these discretization schemes use the most simple (and rough) approximation of the first order derivative:

$$y'(i \cdot \chi, k \cdot \tau) = \frac{1}{2\chi} \{y[(i+1)\chi, k \cdot \tau] - y[(i-1)\chi, k \cdot \tau]\} = \frac{1}{2\chi} [pr(i+1) - pr(i-1)], \quad (6)$$

both these FD schemes lead to rather large simulation errors.

2.3. The permanent 4 space steps symmetric discretization (this work)

Starting from the substitution:

$$u = V_{00} + n \cdot y, \text{ leading to: } \dot{u} = n \cdot \dot{y}, \quad u' = n \cdot y', \quad u''' = n \cdot y''', \quad (7)$$

one finds that the differential equation of the KdV pulses propagation is given by the simplified expression:

$$\dot{u} = -u \cdot u' - d \cdot u'''. \quad (8)$$

Additionally, instead of the 2 steps FD approximation (6) of the space first order derivative, it is used a 4 steps approximation:

$$y'(i \cdot \chi, k \cdot \tau) = \frac{1}{12\chi} \{y(i-2) - 8y(i-1) + 8y(i+1) - y(i+2)\}. \quad (9)$$

In this manner, it is obtained (using an averaged value of $pr(i)$) a FD schema using 4 space steps:

$$f(i) = p(i) - \frac{n \cdot \tau}{18\chi} [pr(i+1) + pr(i) + pr(i-1)] \cdot [pr(i-2) - 8pr(i-1) + 8pr(i+1) - pr(i+2)] - \frac{d \cdot \tau}{\chi^3} [pr(i+2) + 2pr(i-1) - 2pr(i+1) - pr(i-2)]. \quad (10)$$

Taking into account the expressions of the series expansions of the first order and of the third order derivatives by means of 2 space steps, and of 4 space steps, respectively (see e.g. [14], p. 162):

$$y'(i \cdot \chi, k \cdot \tau) = \frac{1}{2\chi} \{y[(i+1)\chi, k \cdot \tau] - y[(i-1)\chi, k \cdot \tau]\} - \frac{\chi^2}{6} y'''[i \cdot \chi, k \cdot \tau], \quad (6')$$

$$\text{and: } y'(i \cdot \chi, k \cdot \tau) = \frac{1}{12\chi} \{y(i-2) - 8y(i-1) + 8y(i+1) - y(i+2)\} + \frac{\chi^4}{5!} \cdot y^V(i \cdot \chi, k \cdot \tau), \quad (7')$$

$$y'''(i \cdot \chi, k \cdot \tau) = \frac{1}{2\chi^3} \{y(i+2) - 2y(i+1) + 2y(i-1) - y(i-2)\} - \frac{\chi^2}{4} \cdot y^V(i \cdot \chi, k \cdot \tau), \quad (11)$$

as well as the rather small value of the space step χ , it results that this FD schema (using a 4 steps symmetric discretization) is considerably more accurate (usually more than 10 times) than the previous 2 discretizations.

3. Choice of the Uniqueness Parameters

Besides the intrinsic uniqueness parameters of a Korteweg-de Vries pulse (soliton): the amplitude A (chosen as equal to 2), the 1-D speed inside an ideal (linear and conservative) medium v_{oo} (chosen as 2), the non-linearity parameter n (chosen value 0.1) and the dissipation coefficient d (chosen value 0.2), we used the main following simulation uniqueness parameters:

a) the FD space step $\chi \equiv dx$ (chosen value 0.15), b) the FD time step $\tau \equiv dt$ (measured in Vliegenthart [13] time units $t_V = \frac{\chi}{n \cdot A + 4d/\chi^2}$ [13], where – for the

above indicated values of the basic KdV parameters: $t_V \cong 0.004195152$), c) simulation space x_{\max} , d) initial position of the KdV soliton peak x_{in} (usually chosen value in our simulations: $x_{in}=200$), e) number I of accomplished FD steps (iterations). An important simulation parameter - for the evaluation of the statistical parameters « skewness » and « kurtosis » of the simulated soliton:

$$s = \frac{M_3}{M_2^{3/2}}, \quad k = \frac{M_4}{M_2^2}, \quad (12)$$

where M_n is the statistical momentum of order n of the soliton components [10] - is the area $A(I)$ under the soliton peak, equal initially to A_{in} ; the change of this area after I steps (iterations) is denoted as: $\Delta A(I) [= A(I) - A_{in}]$. Another parameter whose values indicate the distortions magnitude in the I -th iteration, for the FD

site of index i , is the difference $\delta y_I(i \cdot \chi)$ between the simulated soliton component $y_I(i \cdot \chi)$ and the true (physical) value

$$y(i \cdot \chi, I \cdot \tau) : \delta y_I(i \cdot \chi) = y_I(i \cdot \chi) - y(i \cdot \chi, I \cdot \tau). \quad (13)$$

Of course, for a global characterization of all distortions intervened after I simulation steps, the main parameter is the square mean error $\varepsilon = \langle \delta y_I^2(i \cdot \chi) \rangle$ of the simulated values relative to the true ones of the studied soliton components.

The effective value of the KdV soliton speed is given by the expression :

$$V_{eff.} = V_{oo} + \frac{n \cdot A}{3} ; \quad (14)$$

for the above indicated numerical values, the effective speed is: $V_{eff} \cong 2.0666\dots$

4. Main obtained results and their interpretation

4.1. The general time-space representation of the simulated soliton

A general time-space representation of the simulated (by the numerical schema involving 4 space steps) soliton propagation is presented by Fig. 1.

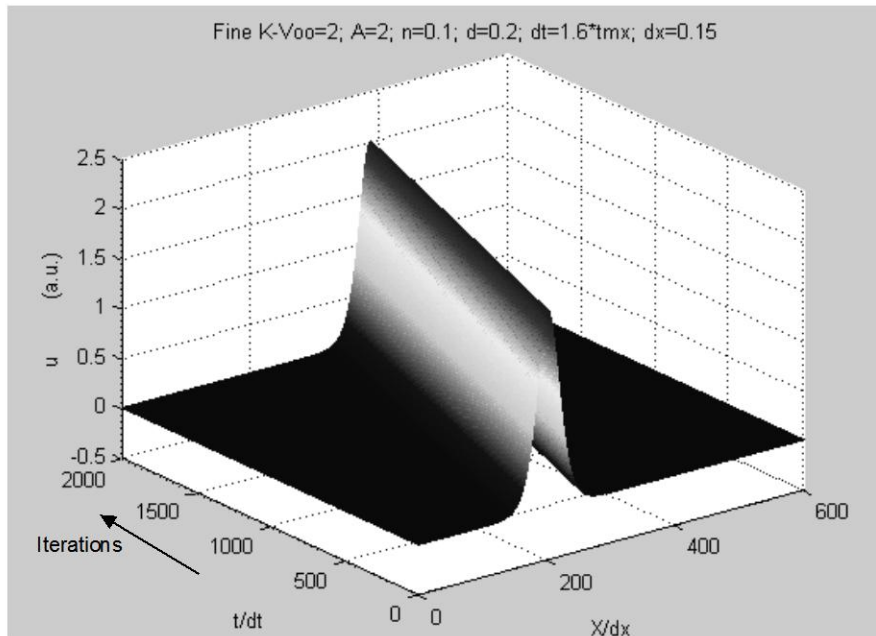


Fig. 1. Space-time representation of a KdV soliton propagation (the numerical values of the soliton shape and dynamic parameters, and those of the used FD simulation are written in this figure top).

In order to check both figure 1 and the above indicated theoretical model, we can estimate the soliton displacement along the OX axis during $I = 2000$ time steps:

$$i = \frac{V_{eff} \times I \times dt}{dx} = \frac{2.066... \times 2000 \times 1.6 \times 0.004195152}{0.15} \cong 184.96 \text{ space steps, in}$$

agreement with figure 1.

4.2. Appearance of distortions

Using the same values of the basic KdV parameters and of the FD simulation, we obtained the figure 2, involving the plot (in red) of the propagated soliton after the first ($I = 3$) time step, and of the corresponding distortion $\delta y_3(i \cdot \chi)$.

The amplitudes of distortions were multiplied by 10^6 to become visible.

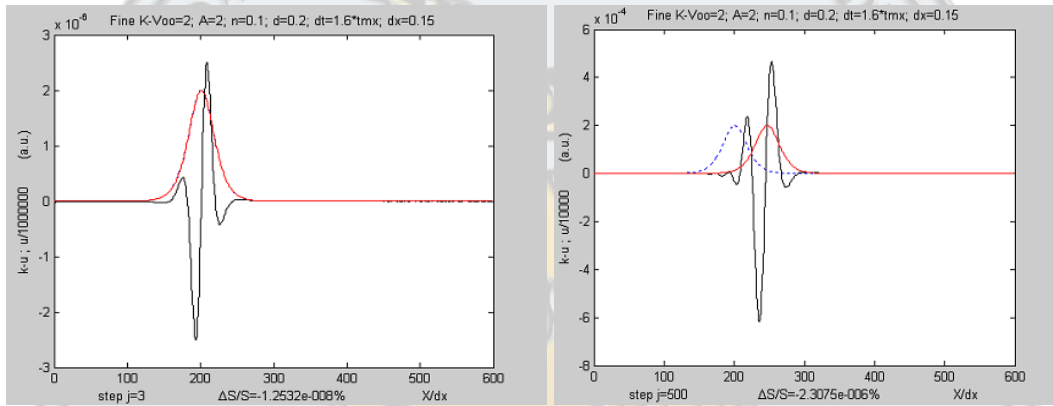


Fig. 2. The simulation begins with the step $I \equiv j = 3$, **Fig. 3.** The black plot indicates the distortions the first 2 iterations being injected analytically.

We ask readers to observe that the distortions begin with the first simulation iteration

($\times 10^4$) for the iteration $I = 500$, while the blue and red plots correspond to the initial and present ($I = 500$) soliton positions, resp.

4.3. Spreading and multiplication of distortions

Figures 3 and 4 present the simulations of the KdV soliton propagation for the iterations $I = 500$ and $I = 2000$, respectively, as well as the corresponding distortions (multiplied by 10^6), while figure 5 presents only the backward part of distortions for the iteration $I = 2500$.

One finds that the pointed out distortions remain considerably weaker than the soliton components, but the number of distortions cycles (somewhat similar to a damped oscillation) increases considerably with the number of accomplished simulation iterations.

Figures 6 and 7 present the same artifacts for both studied discretizations: the permanently 4 space steps discretization and the Landau-Pàez one.

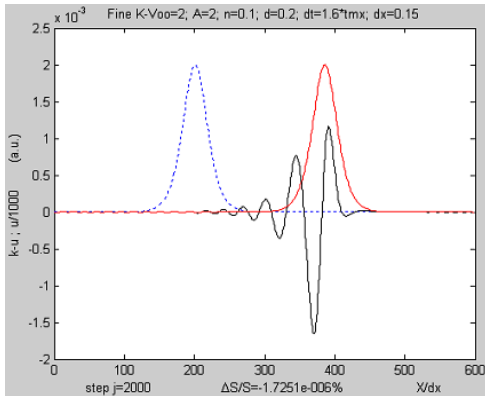


Fig. 4. For the iteration $I = 2000$, one finds both the soliton advance and the rise of distortions amplitude and number of cycles in the backward part of the soliton propagation.

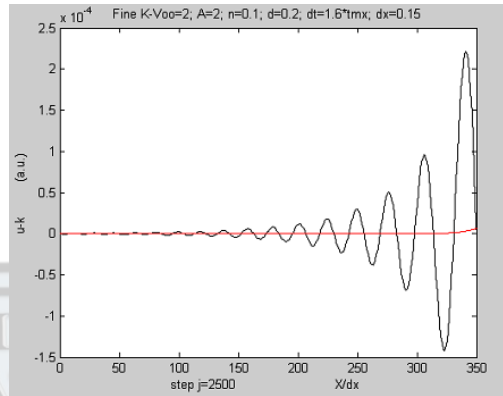


Fig. 5. For the iteration $I = 2500$, one finds that the distortions remain considerably smaller than the soliton amplitude, but the number of their (damped) cycles increase in the backward part.

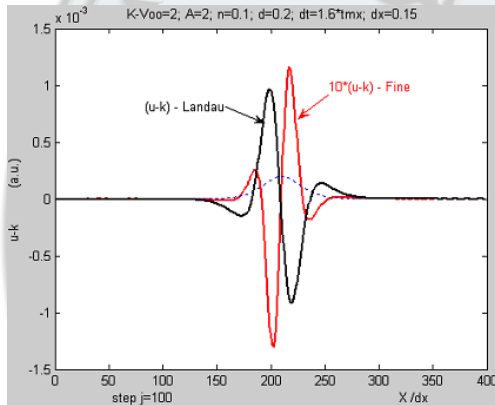


Fig. 6. Comparison of the distortions for the Landau-Pàez (black plot) and of the permanent 4 space steps discretization (red plot), respectively, corresponding to the iteration $j = 100$.

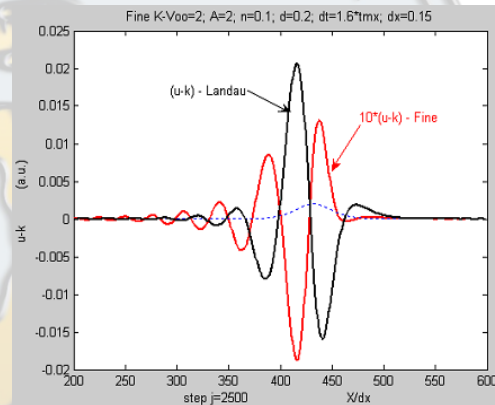


Fig. 7. Comparison of the spreading and multiplication of the distortions for the Landau-Pàez and of the permanent 4 space steps discretization, respectively, for the iteration $j = 2500$.

4.4. Dependencies of the relative square mean simulation error due to distortions on the number of accomplished iterations and the simulation space

The above indicated results point out the increase of distortions amplitude with the number of accomplished FD iterations. Figures 8 and 9 present the plots of the relative square mean simulation error ε corresponding to different values of the time step $\tau \equiv dt$, both for the 4 steps FD scheme and for the Landau-Pàez scheme (see above). One finds: a) the considerably better accuracy of the 4 steps FD scheme relative to the Landau-Pàez scheme (values of ε more than 10 times less for the 4 steps FD scheme), b) the abrupt rise (of burst type, leading to instability) of the relative square mean error ε for values of the time step equal to (or larger) than $1.8 t_V$.

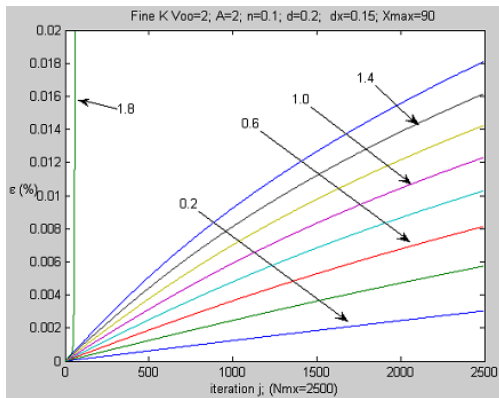


Fig. 8. Plots of the relative square mean error ε versus the number of accomplished iterations for different values of the time step $\tau \equiv dt$ in Vliegenthart time t_V and the 4 steps FD scheme.

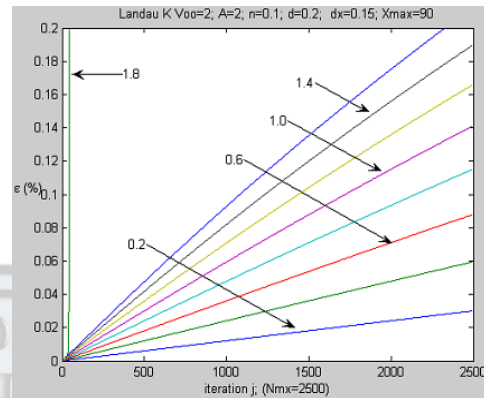


Fig. 9. The same plots in the same conditions, but for the Landau-Pàez FD discretization schema. One finds that the values of the relative square mean error are more than 10 times larger.

Depending on the magnitude x_{\max} of the simulation space, the number of iterations corresponding to the launching of the «burst» phase of the distortions increases quickly (see Figures 10 and 11). In this phase, the square mean simulation error ε remains considerably less for the permanently 4 space steps discretization than for the Landau-Pàez one.

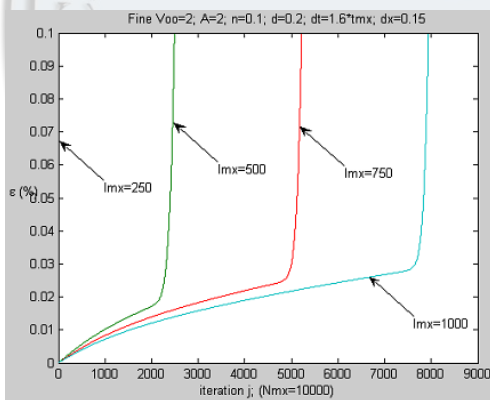


Fig. 10. Plots of the relative square mean error ε versus the number of accomplished iterations for the permanently 4 space steps discretization and different values of simulation space $I_{\max} \equiv x_{\max}$

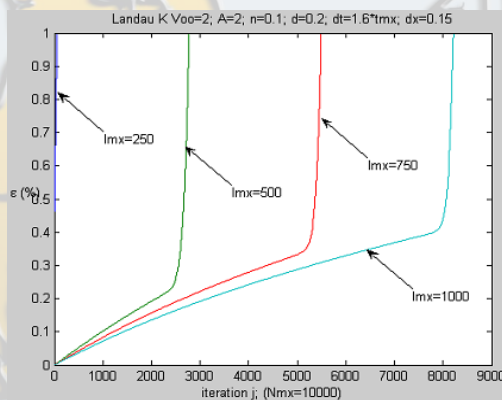


Fig. 11. The same plots in the same conditions, for the Landau-Pàez FD discretization schema. One finds that the values of the relative square mean error are of about 10 times larger.

Finally, for very large values of the iterations number $I \equiv j$ (i.e. a huge «logical depth», which is also a Complexity feature), the plots of the relative square mean simulation error ε versus the iteration number reach a «saturation» phase. One finds (see figures 12, and 13) that in the frame of this «saturation» phase, the relative square mean simulation error tends to constant values of the magnitude order of 15÷20%, for both studied discretizations.

As it is to be expected, the limit (« threshold ») values of the relative square mean simulation error decrease considerably (from approximately 35% to only 17.5%) for higher values of the simulation space ($l_{mx} \equiv x_{\max}$ increasing values from 250 to 1000 space steps), due to the reduction of the effects of interaction (reflection) with/on the boundary walls of the simulation space (see figures 12 and 13).

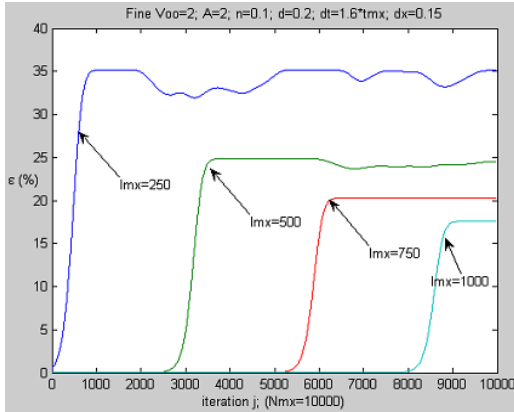


Fig. 12. Plots of the relative square mean error ε versus the number of accomplished iterations for the permanently 4 space steps discretization and different values of simulation space $l_{mx} \equiv x_{\max}$ for the “saturation” phase (huge logical depth).

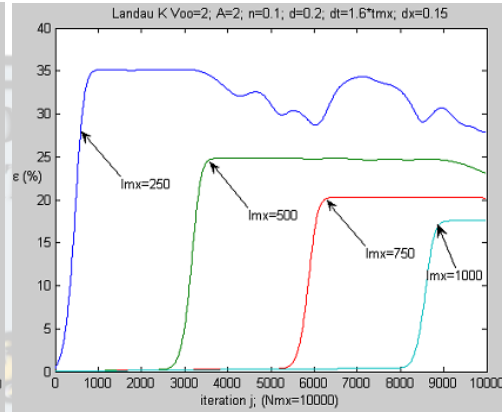


Fig. 13. The same plots in the same conditions, for the Landau-Pàez FD discretization schema. One finds that the values of the relative square mean error are almost the same as those for the permanently 4 space steps discretization.

One can find also that the numbers of iterations corresponding to the launch of the burst phase (figure 14) and the « threshold » (limit) values of the relative square mean simulation errors, reached in the « saturation » phase are practically the same for both studied FD discretizations.

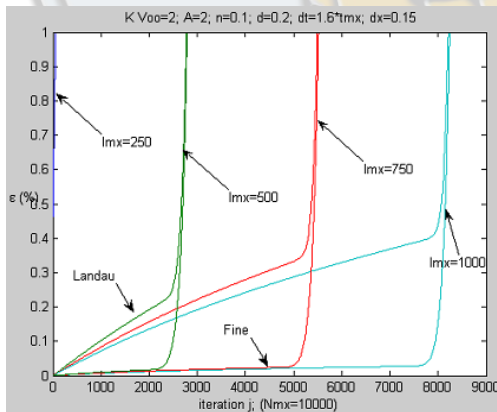


Fig. 14. Plots of the relative square mean error ε versus the number of accomplished iterations for the permanently 4 space steps discretization and for the Landau-Pàez discretization scheme for the “burst” phase launch.

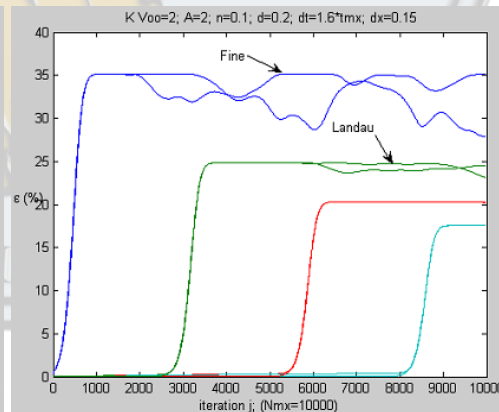


Fig. 15. The same plots for both studied FD discretization schemes, corresponding to the “saturation” phase. One finds that the limit values of the relative mean errors are almost the same for both these discretization schemes.

5. Study of the deformations of the simulated solitonic pulses shape

In order to point out some specific deformations of the FD simulated solitonic pulses shape, there were calculated the moments of their components $y_I(i)$ in the I -th iteration:

$$M_{0I} = \sum_{i_{\min}}^{i_{\max}} y_I(i), \quad M_{1I} = \sum_{i_{\min}}^{i_{\max}} i \cdot y_I(i), \quad (15)$$

and starting from the coordinate of « weight-center » of the simulated solitonic pulse components:

$$\langle i \rangle_I = M_{1I} / M_{0I}, \quad (16)$$

the « centered » moments of the second, third and fourth order were also calculated:

$$M_{2I} = \sum_{i_{\min}}^{i_{\max}} (i - \langle i \rangle_I)^2 \cdot y_I(i), \quad M_{3I} = \sum_{i_{\min}}^{i_{\max}} (i - \langle i \rangle_I)^3 \cdot y_I(i), \quad M_{4I} = \sum_{i_{\min}}^{i_{\max}} (i - \langle i \rangle_I)^4 \cdot y_I(i). \quad (17)$$

In this manner, it is possible to obtain the values of the skewness and kurtosis parameters for the I -th iteration:

$$s_I = \frac{M_{3I}}{M_{2I}^{3/2}}, \quad k_I = \frac{M_{4I}}{M_{2I}^2}. \quad (12)$$

While for the non-deformed (symmetric) launched KdV soliton: $s_0 = 0$ and: $k_0 \cong 4.2$, after several iterations both $|s_I|$ and $|k_I - k_0|$ increase. As it is well-known, the non-null values of the skewness s correspond to asymmetric pulse, the reduced values of kurtosis k correspond to flattened pulses, etc. (see figures 16).

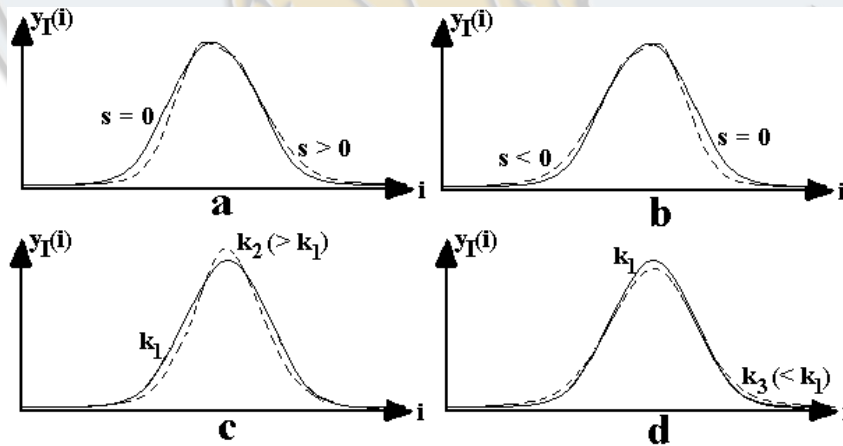


Fig. 16. Comparison of the dotted plots corresponding to FD simulated KdV solitons with the continuous plots for the true (physical) KdV solitons, for different values of the skewness and kurtosis parameters, respectively.

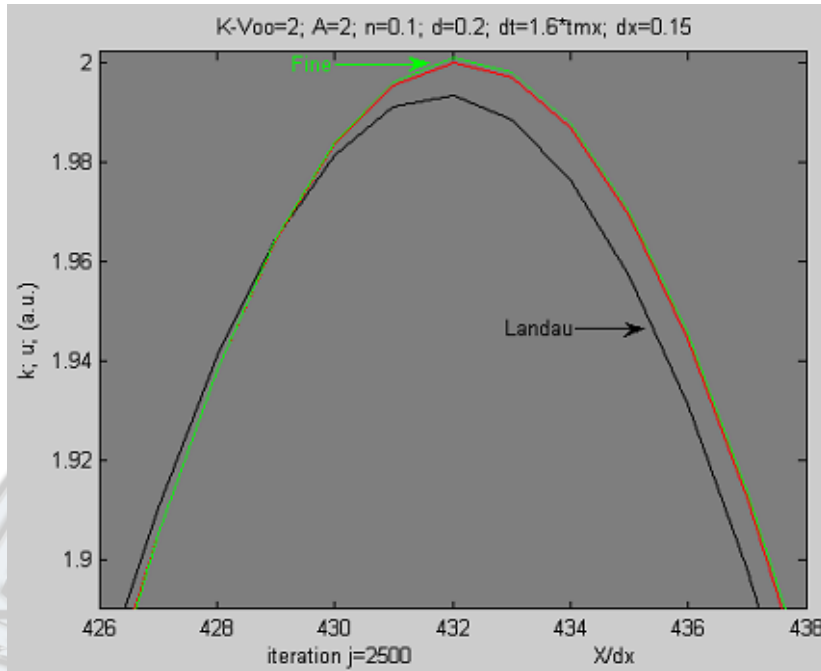


Fig. 17. Comparison of the plots for the Landau-Pàez and permanently 4 space steps discretization schemes, with the red plot of true (physical) KdV soliton.

Taking into account that for not too large numbers of iterations, the changes of skewness and kurtosis are rather small: $|s_I| \ll 1$ and: $|k_I - k_0| \ll 1$, figure 17 presents only the top of the KdV simulated and true, resp. solitonic pulse in order to point out the changes of its shape and compare the results of the permanently 4 space steps FD discretization with those of the Landau-Pàez one. One finds again that the 4 space steps discretization leads to more accurate FD simulations.

6. From the numerical artifacts to the numerical phenomena

As it was shown already (see e.g. [4]), the detailed explanation of the mathematical mechanisms of the new found numerical artifacts (which transform these artifacts in numerical phenomena) is generally very intricate. As it can be expected, the corresponding difficulties are even higher for nonlinear physical systems. For this reason, we will examine here only the mechanism of the distortions appearance, beginning with the first iteration of the FD simulations.

From the expression of the solution of the Korteweg-de Vries equation (1):

$$y = A \cdot \cosh^{-2} \Phi, \text{ where: } \Phi = \xi \left[x - \left(V_{00} + \frac{n \cdot A}{3} \right) \cdot t \right] \text{ and: } \xi = \sqrt{\frac{n \cdot A}{12d}}, \quad (15)$$

it results that:
$$y''' = 8A\xi^3 \sinh \Phi (3 \cosh^{-5} \Phi - \cosh^{-3} \Phi), \quad (16)$$

and:
$$y^V = -16A\xi^5 \sinh \Phi (2 \cosh^{-3} \Phi - 30 \cosh^{-5} \Phi + 45 \cosh^{-7} \Phi) . \quad (17)$$

The distortions amplitude $\delta y_I(i \cdot \chi) = y_I(i \cdot \chi) - y(i \cdot \chi, I \cdot \tau)$ [defined by the expression (13)] involves the contributions of the corrections of the: (i) time derivative:

$$\delta y_{dy/dt} = -\frac{\tau^3}{3} \cdot p\ddot{r}(i) , \quad (18)$$

(ii) nonlinear term δy_n , and of the: (iii) dissipation term:

$$\delta y_d = -\frac{d\chi^2}{4} \cdot pr^V(i) . \quad (19)$$

While the expressions of the corrections of the time derivative and of the dissipation term, respectively, coincide both for the Landau-Pàez and for the permanently 4 steps discretizations:

$$\delta y_{dy/dt} = -\frac{8\xi^3 \tau^3}{3} \left(\frac{n \cdot A}{3}\right)^3 \cdot A \sinh \Phi (3 \cosh^{-5} \Phi - \cosh^{-7} \Phi) \quad (18')$$

(being of the magnitude order of 10^{-10} for the chosen input data, see paragraph 3), and:

$$\delta y_d = \frac{n\xi^5 \chi^2 \tau}{3} \cdot A \sinh \Phi (2 \cosh^{-3} \Phi - 30 \cosh^{-5} \Phi + 45 \cosh^{-7} \Phi) \quad (19')$$

(magnitude order 2×10^{-6} for the chosen input data), the expressions, magnitude order and signs of the contribution δy_n of the nonlinear term are different for the Landau-Pàez and for the (permanently) 4 steps discretization scheme, respectively:

$$\delta y_{LPn} = -\frac{8n\xi^3 \chi^2 \tau}{3} \cdot A \sinh \Phi (3 \cosh^{-5} \Phi - \cosh^{-7} \Phi) \quad (20)$$

(negative, of the magnitude order 4×10^{-6} for the chosen input data), and:

$$\delta y_{4n} = -\frac{8n\xi^5 \chi^4 \tau}{45} \cdot A \sinh \Phi (2 \cosh^{-3} \Phi - 30 \cosh^{-5} \Phi + 45 \cosh^{-7} \Phi) , \quad (20')$$

also negative but of the magnitude order of only 10^{-10} .

One finds so that the dominant distortions term is the (negative) nonlinear term δy_{LPn} (20) for the Landau-Pàez discretization and the dissipation term δy_d (19') for the permanently 4 space steps discretization scheme.

From the above expressions, one finds that: $\delta y_1(i) = 0$ for $\sinh \Phi = 0$, hence for:

$x = \left(V_{oo} + \frac{nA}{3} \right) \cdot t$, i.e. for the peak of the simulated soliton, in agreement with figures 2 - 7. Additionally, it results that at the right of the soliton's peak, i.e. for $\Phi > 0$ we have: $\delta y_{4steps}(i) > 0$ and $\delta y_{LP}(i) < 0$ and – at the left of the soliton's peak, i.e. for $\Phi < 0$: $\delta y_{4steps}(i) < 0$, $\delta y_{LP}(i) > 0$, again in agreement with figures 2 - 7.

Taking into account that for the Landau-Pàez discretization the extreme values of distortions occur then for extreme values of y''' , and the fourth order derivative of y is:

$$y^{IV} = 8A\xi^4 \left(2 \cosh^{-2} \Phi - 15 \cosh^{-4} \Phi + 15 \cosh^{-6} \Phi \right), \quad (21)$$

it results that these extremes correspond approximately to the solutions of the equation:

$$15x^2 - 15x + 2 = 0, \text{ where: } x = \cosh^{-2} \Phi.$$

One obtains: $\cosh \Phi = \sqrt{\frac{30}{15 + \sqrt{105}}} \cong 1.09007$, hence: $e^\Phi \cong 1.09007 \pm 0.433892$ and:

$\Phi_{\max/\min} = \pm 0.4213165$. Because for the used numerical values, the pseudo-wave-vector ξ (see equation (16c)) is: $\xi \approx 0.2887$, the relative (in respect with the KdV soliton's peak) locations $i_{\max/\min}$ of the maximum and minimum of the Landau-Pàez discretization distortion, respectively, are given by the relation:

$$\left[x - \left(V_{oo} + \frac{nA}{3} \right) \cdot t \right]_{extr.} = \frac{\Phi_{\max/\min}}{\xi} \cong \pm 1.46005,$$

hence: $\Delta i_{\max/\min} = \frac{[x - (V_{oo} + nA/3) \cdot t]}{dx}$ somewhat less than 10, again in agreement with Figure 6 and 7.

As it concerns the position of the second “node” of the initial distortions (see figures 2 and 6), it is given for the Landau-Pàez discretization by the condition: $3 \cosh^{-5} \Phi - \cosh^{-3} \Phi = 0$, hence: $\cosh \Phi_{2LP} = \sqrt{3}$, and:

$$e^{\Phi_{2LP}} = \sqrt{3} + \sqrt{2}, \text{ obtaining: } \Phi_{2LP} \cong 1.146216.$$

Finally, one obtains the relative (in respect with the KdV soliton peak location) position of the second “node” ($\delta y_1(i) = 0$) of the initial distortion:

$$\Delta i_{2nd\ nodes, LP} = \frac{\Phi_{2LP}}{\xi \cdot dx} (\approx 26.4684 \text{ for the used numerical values}).$$

One finds again the agreement with the simulation results presented by figure 6.

Similarly, for the permanent 4 space steps discretization, the position of the second “node” of the initial distortions is given by the condition:

$$2 \cosh^{-2} \Phi - 15 \cosh^{-4} \Phi + 15 \cosh^{-6} \Phi = 0,$$

leading to the equation: $2y^2 - 30y + 45 = 0$, where: $y = \cosh^2 \Phi$. (22)

The solution of the equation (22) is: $\Phi_2 \cong 0.756676$, leading to:

$$\Delta i_{2nd\ nodes} = \frac{\Phi_2}{\xi \cdot dx} (\approx 17.4732 \text{ for the used numerical values}).$$

One finds that the first oscillation of the distortions of the permanent 4 space steps discretization is sensibly narrower than the corresponding one of the Landau-Pàez discretization, again in agreement with figure 6.

Of course, the accurate quantitative explanation of all pointed out numerical artifacts requires a rather difficult¹ additional study.

7. Conclusions

A new permanently 4 FD space steps discretization was proposed and its numerical artifacts were systematically studied (for several uniqueness parameters of the studied solitons and simulations) and compared with those of the Landau-Pàez «classical» discretization. Despite of the well-known difficulties of the numerical artifacts examination, the accomplished study succeeded to point out the possibility to explain quantitatively the mechanism of several numerical artifacts, which can be considered so as numerical phenomena.

Taking into account the huge numbers of solitons applications [18], [19], and the efficiency of numerical simulations, the newly obtained results are useful for the improvement of the accuracy of FD simulations of the solitons propagation.

¹We will mention that many problems in the field of Numbers Theory are extremely difficult. E.g., the statement of the (Pierre de) *Fermat's last (greatest) theorem* was published in 1670 [15], by his eldest son – Clément Samuel Fermat, but its solution was found only in 1995 [16] by the American professor Andrew Wiles. Wiles describes ([17], p. 236) his experience of doing mathematics in terms of a journey through a dark unexplored mansion: “One enters the first room of the mansion and it’s dark. Completely dark. One stumbles around bumping into the furniture, but gradually you learn where each piece of furniture is. Finally, after six months or so, you find the light switch, you turn it on, and suddenly it’s all illuminated. You can see exactly where you were. Then you move in the next room and spend another six months in the dark. So each of these breakthroughs, while sometimes they’re momentary, sometimes over a period of one day or two, they are the culmination of, and couldn’t exist without, the many months of stumbling around in the dark that precede them”.

REFERENCES

- [1] R. Skeel, in *SIAM News*, vol. 25, no. 4, 1992, p. 11.
- [2] a) *** *SIAM News*, vol. 29, no. 8, 1996, p. 1, 123.
b) J. L. Lions *Ariane 5, Flight 501 Failure, 1996* in
<http://www.ima.umn.edu/~arnold/disasters/ariane5rep.html>
c) <http://www.siam.org/siamnews/general.ariane.htm>
- [3] D. W. McClure, *Computer Rounding Errors. Basic Notions*, in E. Bodegom et al “Computational Physics Guide”, vol. 1 “Basic Notions”, Politehnica Press, Bucharest, 2009, p. 122.
- [4] D. Iordache, *Contributions to the study of Numerical Phenomena intervening in the Computer Simulations of some Physical Processes*, Credis Printing House, Bucharest, 2004.
- [5] D. A. Iordache, A. Petrescu, V. Iordache, *Study of the solitons propagation through optical fibers*, in *UPB Sci. Bull. A*, vol. 72, no. 1, 2010, pp. 53-58.
- [6] A. Petrescu, A. R. Sterian, P. E. Sterian, *Solitons Propagation in Optical Fibers Computer Experiments for Students Training*, in *Lecture Notes in Computer Science*, vol. 4705, 2007, pp. 450-461.
- [7] R. Dobrescu, D. Iordache, *Complexity and Information*, Romanian Academy Printing House, Bucharest, 2010.
- [8] D. A. Iordache, Șt. Pușcă, C. Toma, *Numerical Analysis of some Typical FD Simulations of the Waves Propagation through Different Media*, in *Lecture Notes in Computer Science*, vol. 3482, 2005, pp. 614-620.
- [9] D. J. Korteweg, G. de Vries, *On the Change of Form of Long Waves Advancing in a Rectangular Canal and on a New Type of Long Stationary Waves*, in *Phil. Mag.*, vol. 36, 1895, pp. 422-443.
- [10] E. Bodegom, D. W. McClure, P. P. Delsanto, A. S. Gliozzi, D. A. Iordache, F. Pop, C. Roșu, and R. Widenhorn, *Computational Physics Guide*, Politehnica Press, Bucharest, 2009.
- [11] R. H. Landau, M. K. Pàez, *Computational Physics. Problem solving with computers*, John Wiley, 1997.
- [12] D. Iordache, *Selected Works of Numerical Physics*, Printech, Bucharest, 2000.
- [13] a) A. C. Vliegthart, in *J. Eng. Math.*, vol. 3, 1969, pp. 81-94;
b) A. C. Vliegthart, in *J. Eng. Math.*, vol. 5, 1971, pp. 137-155.
- [14] D. Iordache, *Numerical Methods in Optical Engineering* (in Romanian), Politehnica Press, Bucharest, 2010.
- [15] Cl. S. Fermat, *Diophantus' Arithmetica containing (48) observations by P. de Fermat*, Toulouse, 1670.
- [16] A. Wiles *Modular elliptic curves and Fermat's last theorem*, in *Annals of Mathematics*, vol. 142, 1995, pp. 443-551.

[17] S. Singh, *Fermat's Enigma: the Epic Quest to Solve the World's Greatest Mathematical Problem*, Walker Publishing Company, New York, 1997.

[18] Y. S. Kishvar, G. P. Agrawal, *Optical Solitons: from Fibers to Photonic Crystals*, Academic Press, New York, 2003.

[19] L. Munteanu, St. Donescu, *Introduction to Soliton Theory: Applications to Mechanics*, Book Series Fundamental Theories of Physics, vol. 143, Kluwer Academic Publishers, 2004.

